Published in final edited form as:
Biochemistry. 2005 January 18; 44(2): 480–489.

Microsomal Glutathione *S*-Transferase 1 in the Retinal Pigment Epithelium: Protection against Oxidative Stress and a Potential Role in Aging[†,‡]

Akiko Maeda[§], **John W. Crabb**[‖], and **Krzysztof Palczewski**[*,§,⊥,#]
Departments of Ophthalmology, Pharmacology, and Chemistry, University of Washington, Seattle, Washington 98195, and Cole Eye Institute, Cleveland Clinic Foundation, 9500 Euclid Avenue, Cleveland, Ohio 44195

Abstract

High oxygen tension, exposure to light, and the biochemical events of vision generate significant oxidative stress in the retina and the retinal pigment epithelium (RPE). Understanding the mechanisms and basis of susceptibility to progressive retinal diseases involving oxidative damage such as age-related macular degeneration (AMD) remains a major challenge. Here microsomal glutathione *S*-transferase (MGST1) is shown to be a dominant, highly expressed enzyme in bovine and mouse RPE microsomes that displays significant reduction activity toward synthetic peroxides, oxidized RPE lipids, and oxidized retinoids. This enzymatic reduction activity (GPx) can be partially neutralized with a monoclonal anti-MGST1 antibody developed in this study. MGST1-transfected HEK293 cells exhibited greater viability (70 ± 4% survival) compared with untransfected control cells (46 ± 4% survival) when challenged with 20μM H_2O_2, and greater viability of MGST1-transfected cells following challenge with oxidized docosahexaenoic acid was also observed. Cultured ARPE19 cells transfected with silencing MGST1 siRNAs exhibited lower expression of MGST1 (12% and 26% of the controls) and significantly lower GPx activity (44 ± 13%) and, thus, were more susceptible to oxidative damage. Immunoblotting revealed that the in vivo expression of MGST1 in mouse RPE decreases 3–4-fold with age, to trace levels in 18-month-old mice. GPx activity in the RPE was also found to be reduced in 12-month-old mice to ~67%. These results support an important protective function for MGST1 against oxidative insult in the RPE that decreases with age and suggest that this enzyme may play a role in the development of age-related diseases such as AMD.

Aging of the retinal pigment epithelium (RPE)[1] involves many biochemical changes and alterations in the kinetics of physiological renewal of the photoreceptor cells. The apparent

[†]This research was supported by NIH Grants EY09339, EY13385, EY06603, and EY14239, a grant from Research to Prevent Blindness, Inc. (RPB), to the Department of Ophthalmology at the University of Washington, the Stargardt and Retinal Eye Disease Fund, and a grant from the E. K. Bishop Foundation. K.P. is a RPB Senior Investigator.

[‡]GenBank Accession Number AY334548.

* Address correspondence to this author at the Department of Ophthalmology, University of Washington, Box 356485, Seattle, WA 98195-6485. Phone: 206-543-9074. Fax: 206-221-6784. E-mail:palczews@u.washington.edu..
[§]Department of Ophthalmology, University of Washington.
[‖]Cole Eye Institute, Cleveland Clinic Foundation.
[⊥]Department of Pharmacology, University of Washington.
[#]Department of Chemistry, University of Washington.

[1]Abbreviations: AMD, age-related macular degeneration; CEP, ω-(2-carboxyethyl)pyrrole; CDNB, 1-chloro-2,4-dinitrobenzene; (c)-GST, (cytosolic) glutathione *S*-transferase; DHA, docosahexaenoic acid; DM, dodecyl β-maltoside; DMSO, dimethyl sulfoxide; GPx, glutathione peroxidase; GR, glutathione reductase; GST, glutathione *S*-transferase; GSH, reduced glutathione; GSSG, oxidized glutathione; 13(*S*)-HpODE, 13(*S*)-hydroperoxy-9(*Z*),11(*E*)-octadecadienoic acid; mAb, monoclonal antibody; MDA, malondialdehyde; MGST1, microsomal glutathione *S*-transferase 1; MTT, 3-(4,5-dimethylthiazol-2-yl)-2,5-diphenyltetrazolium bromide; pAb, polyclonal antibody; ROS, rod outer segment-(s); RPE, retinal pigment epithelium; TBARS, thiobarbituric acid-reactive substances.

transformations in the RPE involve changes in and loss of intact melanin granules, as well as accumulation of the intracellular phototoxic lipofuscin. This pigment, composed of oxidized lipids and retinoids plus highly conjugated proteins, is linked to several oxidative changes, some leading to apoptosis and a gradual decline in the number of the RPE cells (*1*). In severe cases this process may lead to age-related macular degeneration (AMD). AMD is a degenerative disease of the macular photoreceptors, the RPE, and Bruch's membrane. It is the leading cause of irreversible blindness in elderly people in developed countries (*2*). The cause of AMD is not well understood, and rigorous studies related to the function of the RPE are required in order to develop effective treatment.

The RPE is affected by environmental factors, particularly intense and long-term exposure to light, which can induce damage to both the retina and the RPE (*3*). The greatest susceptibility to this type of injury arises in animals exposed to light at night, suggesting a circadian-dependent, oxidation-induced loss of photoreceptor cells. The continuous exposure of the RPE and photoreceptors to light, the large consumption of oxygen by these cells, a significant daily shedding of the photoreceptor cells and subsequent phagocytosis by the RPE, and substantial levels of docosahexaenoate (DHA)-containing lipids and retinoids in the retina are all exacerbating factors in free radical formation and retinal oxidative injury. Light-induced oxidative damage to the retina and the RPE has been the subject of many recent studies. For example, the antioxidant ascorbic acid, which is abundant in the retina but decreases during intense light exposure (*4*), appears to help to alleviate retinal light damage (*5*). The pathways of retinal oxidative damage remain to be determined; however, evidence supports the involvement of highly oxidizable retinoids and lipids. UV light can induce aggregation and loss of activity of the retinal ATP-binding cassette transporter in the presence of all-*trans*-retinal in vitro (*6*) and enhances the rate of RPE microsomal-catalyzed reverse isomerization of 11-*cis*-retinol (and 13-*cis*-retinol) to all-*trans*-retinol (*7*). Dietary vitamin A-depleted rats as well as animals with impaired visual cycle proteins are more resistant to light damage than normal control animals (*8–10*). Free radical-induced oxidation of DHA-containing lipids generates ω-(2-carboxyethyl)pyrrole (CEP) protein adducts that are more abundant in ocular tissues and plasma from AMD patients than normal human donors and appear to contribute to the pathogenesis of AMD (*11*, *12*). A hydroxylation product of DHA, 10,17(*S*)-docosatriene (neuroprotectin D1), potently counteracts H_2O_2/necrosis factor α oxidative stress-triggered apoptotic RPE DNA damage (*13*).

Glutathione *S*-transferases (GSTs) are one of several detoxification enzymes. GSTs are divided into two evolutionarily distinct families: the cytosolic, soluble enzymes and the membrane-associated proteins in eicosanoid and glutathione metabolism (MAPEG). In total, 20 human cytosolic and 5 membrane-bound enzymes have been identified (*14*). The cGSTs are further subdivided into several divergent classes: α, μ, ω, π, θ, and ξ isoenzymes have been described in mammals, π, τ, and λ isoenzymes are expressed in plants, Δ is present in insects, and β isoenzyme is present in bacteria (*15–19*). Representatives from most classes of soluble GSTs have been well studied and shown to have glutathione *S*-transferase, peroxidase, and isomerase activities. GSTs are expressed at elevated levels in tumor cells, inadvertently increasing the chemotherapeutic resistance of these cells (*20*). MGST1 belongs to the MAPEG superfamily. At present, other mammalian members of MAPEG include two glutathione *S*-transferase/peroxidases (MGST2 and MGST3), 5-lipoxygenase activating protein, leukotriene C4 synthase, and the closest relative to MGST1, microsomal PGE2 synthase (*21*). MGST1 functions as a glutathione *S*-transferase and as a peroxidase, thus potentially protecting cells from reactive components and oxidative stress (*22*). MGST1 is an ER-bound enzyme (*17*) that forms a functional homotrimer (*23*, *24*). Its polypeptide chain of 155 amino acids traverses the ER membrane four times, with both N- and C termini facing the lumen of the ER (*24*).

Toward the identification and characterization of dominant RPE proteins, bovine RPE was used as an immunogen to generate monoclonal antibodies (mAbs) by hybridoma techniques. Microsomal glutathione *S*-transferase 1 (MGST1) was identified as one of the immunogens, and in subsequent analyses we confirmed the abundant expression of this enzyme in the RPE. Here we demonstrate that MGST1 is one of the most active detoxification enzymes of the RPE. In addition, we observed a gradual decline in the expression of MGST1 in mouse RPE with age, suggesting a possible correlation with progressive age-related retinal diseases associated with oxidative injury such as age-related macular degeneration.

MATERIALS AND METHODS

Chemicals and Antibodies

Bovine liver cGST, reduced glutathione (GSH), oxidized glutathione (GSSG), glutathione reductase (GR), all-*trans*-retinal, all-*trans*-retinol, retinyl palmitate, 1-chloro-2,4-dinitrobenzene (CDNB), NADPH, 3-(4,5-dimethylthiazol-2-yl)-2,5-diphenyltetrazolium bromide (MTT), dimethyl sulfoxide (DMSO), octadecane, and poly-(ethylene glycol) (PEG, MW 1500) were purchased from Sigma (St. Louis, MO). 13(*S*)-Hydroperoxy-9(*Z*),11(*E*)-octadecadienoic acid [13(*S*)-HpODE] was obtained from Cayman Chemical Co. (Ann Arbor, MI). Actin pAb and α-tubulin pAb were obtained from Santa Cruz Biotechnology, Inc. (Santa Cruz, CA). Anti-RPE65 pAb were generated in rabbits against bacterially expressed RPE65 protein using a method described previously (*25*).

Preparation of Bovine RPE Microsomes

Fresh bovine eyes were obtained from a local slaughterhouse (Schenk Packing Co., Inc., Stanwood, WA). RPE microsomes and ROS were prepared as described previously (*26*, *27*). Microsomes were suspended in 10 mM 3-(*N*-morpholino)-propanesulfonic acid (pH 7.0) containing 1 μM leupeptin and 1 mM dithiothreitol at a protein concentration of ~5 mg/mL as determined by the Bradford method (*28*). Aliquots were stored at −80 °C and were typically used within 1 month of preparation.

H_2O_2 Treatment of Samples

For the H_2O_2 treatment of the RPE, retinoids, and DHA, 10 μL of 30% H_2O_2 was added to the 200 μL aliquots of the substrate and incubated for 10 min on ice. H_2O_2 was removed by evaporation on the Speed-Vac. To ensure complete removal of residual amounts of H_2O_2, the pellet was treated three to four times with freshly added aliquots of ethanol and evaporated each time.

Monoclonal Antibody Production

Monoclonal antibodies were generated by standard techniques as described previously (*29*). As the antigens, RPE microsomes (50 μg) were immunized subcutaneously to 6-week-old female BALB/c mice (The Jackson Laboratory, Bar Harbor, ME). Hybridoma cell lines were prepared by fusion of NS1 mouse myeloma cells (American Type Culture Collection, Manassas, VT) (3×10^7) with splenocytes (1×10^8) from immunized mice using 50% PEG. The culture supernatants from resulting hybridomas were screened with RPE microsomes by immunoblot. Positive hybridomas were subcloned at least three times by the method of limiting dilution in microtiter plates. A1 mAb (1 mg/mL) was used at 1:2000 dilution for the immunoblotting.

SDS–PAGE and Immunoblotting

SDS–PAGE on 12.5% or 15% polyacrylamide gels and Western blotting methods were as described elsewhere (*30*, *31*).

GST and GPx Activity

GST activity toward 1-chloro-2,4-dinitrobenzene (CDNB) was determined spectrophotometrically at 340 nm by the method of Habig et al. (*32*). One unit of GST activity was defined as the amount of enzyme catalyzing the conjugation of 1 μmol of CDNB with GSH per minute at 25 °C. GPx activity toward hydroperoxide substrates was determined using the GR-coupled assay of Yang et al. (*33*). Briefly, the reaction mixture containing 3.2 mM GSH, 0.32 mM NADPH, 1 unit of GR, and 0.82 mM EDTA in 0.16 M Tris (pH 7.0) was preincubated with GST at the amounts indicated in the figure legends at room temperature for 5 min. The total volume was 1 mL. The reaction was started by addition of appropriate hydroperoxide substrates (prepared in methanol). The consumption of NADPH was monitored at 340 nm for 5 min. For the activation of MGST1, membranes were incubated in 0.16 M Tris (pH 7.0) containing 0.1% Triton X-100 and centrifuged at 275000*g* for 20 min; the supernatant was used in the assay. One unit of GPx activity was defined as the amount of enzyme necessary to consume 1 μmol of NADPH/min. Retinoids were extracted from RPE microsomes with 500 μL of hexane, dried with argon, and used as substrates in the assays. A nonsubstrate blank as well as a nonenzyme additional blank was used to correct for non-GR-dependent NADPH oxidation and nonenzymatic peroxidase activity. The results were examined using the one-way ANOVA test.

cDNA Cloning and Sequencing

Total RNA from fresh bovine RPE was isolated using TRIzol reagent according to the manufacturer's protocol, and 2 μg of total RNA was reverse-transcribed using reverse transcriptase with oligo-(dT) primers (Superscript II; Gibco-Life Technologies, Rockville, MD). To obtain the bovine DNA sequence, PCR amplifications were performed using the RT reaction mixture with primer pairs from human MGST1 cDNA and EST database sequences: sense, 5′-TATAGGATCCCTAATGGAGAATGAAGTATTC-3′; antisense, 5′-AATATGCAATGGTGTGGTAG-3′; sense, 5′-GTTTTTGCCAATCCAGAAGA-3′; antisense, 5′-TATAGAGCTCCAGGTACAATTTACTTTTCAG-3′. PCR products were cloned into pCRII-TOPO vector (TOPO TA cloning kit; Invitrogen, Carlsbad, CA) and sequenced by the dideoxy terminator method (ABI-Prism; Perkin-Elmer, Wellesley, MA).

Bacterial and Stable Cell Line Expression of MGST1

For bacterial expression, human MGST1 was amplified from the human RPE cDNA library (a generous gift from Dr. Zack of Johns Hopkins University) by PCR with the primer pair: 5′-TATAGGATCCAAAATGGTTGACCTCACCC-3′ sense and 5′-TATAGAGCTCCAGGTACAATTTACTTTTCAG-3′ antisense primers. PCR products were digested with *Bam*HI and *Sal*I and inserted into pET21a vector (Novagen, Darmstadt, Germany). The T-Rex system (Invitrogen) was used to produce tetracycline-inducible MGST1 cell lines. Briefly, MGST1 cDNA was amplified from the bovine RPE cDNA library with 5′-AAAATGGCCAACCTTTCGCAGC-3′ sense and 5′-TTACAGGTACAGTTTACTCTTCA-3′ an-tisense primers derived from the bovine MGST1 sequence. PCR products were cloned into a pCRII-TOPO vector (TOPO TA cloning kit; Invitrogen) and sequenced by the dideoxy terminator method (ABI-Prism; Perkin-Elmer). MGST1 was excised with *Bam*HI and subsequently treated with the Klenow nuclease fragment. Next, MGST1 cDNA was cut with *Pst*I and cloned into the *Pst*I/*Xho*I site of the pcDNA4 vector. Using MGST1-specific forward and reverse primers, the entire product was sequenced for verification. The plasmid was then transfected using Lipofectamine (Invitrogen) into HEK293 cells (American Type Culture Collection), T-Rex-293, stably expressing the tetracycline repressor. These cells were grown under blasticidin selection. After transfection, zeocin was added to the culture medium, and surviving colonies of cells were isolated and subsequently expanded into six-well plates. HEK293 cells were grown in Dulbecco's modified

Eagle's medium containing high glucose (Invitrogen) at 37 °C in the presence of 5% CO_2. In all of the experiments, the cells expressing MGST1 were harvested after 48 h of induction with tetracycline (1 μg/mL).

Protein Identification by Mass Spectrometry

MGST1 was identified by LC MS/MS utilizing well-established methods (*12*, *34*). Briefly, Coomassie blue-stained gel bands were excised, Coomassie blue was washed away, proteins were digested in-gel with trypsin, and peptides were extracted for mass spectrometric analysis. Liquid chromatography electrospray tandem mass spectrometry (LC MS/MS) was performed using a CapLC system (Waters Corp., Milford, MA) and a quadruple time-of-flight mass spectrometer (QTOF2; Waters Corp., Milford, MA). Protein identifications from MS/MS data utilized Micromass software ProteinLynx Global Server, MassLynx, version 3.5, and the Swiss-Protein and NCBI protein sequence databases.

Cytotoxicity Assay

For the MTT assay, 2×10^4 cells in 190 μL of medium were added to each well of 96-well flat-bottomed microtiter plates. The medium was supplemented with 10 μL of PBS containing various concentrations of H_2O_2. Five replicate wells were used for each concentration of H_2O_2. After treatment with H_2O_2 at 37 °C for 48 h, 10μL of 3-(4,5-dimethylthiazol-2-yl)-2,5-diphenyltetrazolium bromide (MTT) solution (2 mg/mL in PBS) was added to each well, and the plates were incubated for an additional 4 h at 37 °C. The medium was aspirated; next, intracellular formazan dye crystals were dissolved with 100 μL of DMSO at room temperature in the dark. The absorbance of formazan at 560 nm was measured using a microplate reader. The results were examined using the one-way ANOVA test.

DNA Fragmentation

Cells were treated with the indicated concentrations of H_2O_2 in complete medium and washed with 10 mM phosphate (pH 7.5) containing 100 mM NaCl before their genomic DNA was extracted (Genomic DNA extraction kit; QIAGEN, Valencia, CA). DNA samples (1 μg) were loaded on 2% agarose gels containing ethidium bromide. Electrophoresis was carried out for 2 h at 50 V, and gels were visualized under UV light.

Inhibition of MGST1 Expression in Cultured RPE Cells and Hyperoxia Induction in Vitro

Four targeting siRNA sequences within human MGST1 were selected on the basis of criteria proposed by Elbashir et al. (*35*–*37*). F136 represents sequence 5′-AATCCAGAAGACTGTGTAGCA-3′ (position in the gene sequence: 136–157), F143 is 5-AAGACTGTGTAGCATTTGGCA-3′ (position in the gene sequence: 143–164), F172 is 5′-AATGCCAAGAAGTATCTTCGG-3′ (position in the gene sequence: 172–193), and F264 is 5′-AATTGGCCTCCTGTATTCCTT-3′ (position in the gene sequence: 264–285). siRNA was prepared with a Silencer siRNA construction kit (Ambion Inc., Austin, TX) by following the manufacturer's protocol.

Transfection of siRNA to ARPE19 cells (American Type Culture Collection) was performed with the RNAiFect Transfect reagent (QIAGEN) using guidelines provided by the manufacturer. Twenty-four hours after transfection, hyperoxia was induced in the cells by the addition of 30 μM H_2O_2. The results were examined using the one-way ANOVA test.

Analysis of Lipid Peroxidation: Thiobarbituric Acid (TBA) Reactive Substance (TBARS) Assay

Lipid peroxide levels were determined by thiobarbituric acid-reactive substances (TABRS) as described by Wagner et al. (*38*). Cells (3×10^7) were collected by centrifugation at 500*g* for

10 min and washed twice with 10 mM sodium phosphate solution (pH 7.5) containing 100 mM NaCl. The pellet was resuspended in 1 mL of 10 mM potassium phosphate buffer, pH 7.0, containing 0.4 mM butylated hydroxytoluene and vortexed vigorously, and samples were immediately used for TBARS assay. The cellular protein was precipitated by mixing homogenates with 120 μL of saturated trichloroacetic acid solution. After centrifugation at 4000*g* for 15 min, supernatants were transferred to glass test tubes and mixed with 2-thiobarbituric acid solution in 0.1 N NaOH with a final concentration of 3.5 mg/mL (total volume 1 mL). The samples were incubated for 30 min at 75 °C. After the samples were cooled to room temperature, the absorbance of the samples was measured at 535 nm. Lipid peroxidase levels were expressed as picomoles of malonaldehyde per milligram of cell protein. The extinction coefficient used for malonaldehyde was $1.53 \times 10^5\ M^{-1}\ cm^{-1}$.

Extraction of Proteins from Mouse Eyes

Mouse eyes were enucleated, and the anterior segment, vitreous, and retina were carefully removed under a microdissecting microscope. RPE cells were floated by gently scraping eyecups with a fine brush, using 100 μL/eye of 10 mM sodium phosphate solution (pH 7.5) containing 100 mM NaCl. The cell suspension was removed and centrifuged at 275000*g* for 20 min. The pellet was then reconstituted in 10 μL/eye of 10 mM sodium phosphate (pH 7.5) containing 100 mM NaCl.

RESULTS

A1 mAb against a Protein from Bovine RPE Microsomes

To produce monoclonal antibodies against RPE specific proteins, BALB/c mice were immunized with bovine RPE microsomes, and hybridoma cell lines were prepared by fusion of NS1 mouse myeloma cells with immunized mouse splenocytes. Among the hybridoma cell lines, one designated A1 reacted with a 17 kDa protein in bovine RPE microsomes treated with 100 mM Na_2CO_3 (pH 10) to strip away membrane-associated proteins (Figure 1A). Bovine retina and ROS did not cross-react with A1 mAb, suggesting that the expression was largely confined to the RPE. The 17 kDa protein was also detected with A1 mAb in the human ARPE19 cell line (Figure 1B). When soluble proteins and membrane proteins from ARPE19 were separated, the 17 kDa antigen was found only in the insoluble fraction (data not shown). Mouse tissues from several organs including the RPE, whole eye, brain, heart, lung, liver, spleen, kidney, and muscle were homogenized with 100 mM Na_2CO_3 (pH 10) to test for immunoreactivity with A1 mAb. The equivalent size of the samples loaded on the gel was verified by the presence of similar amounts of actin (Figure 1C). MGST1 was abundant in the liver cells as well as in the RPE cells, to an extent not seen in other tested tissues (Figure 1C). In addition, protein extracts from cornea, lens, vitreous, and sclera did not show cross-reactivity (data not shown). The protein solubility profile, including requirement for a detergent and lack of solubility at high pH buffer or in high ionic strength buffers, suggests that the 17 kDa protein may be a transmembrane protein (Figure 1D).

Molecular Identification of the 17 kDa Protein in Bovine RPE Microsomes

Bovine RPE microsomes were washed with 100 mM Na_2CO_3 (pH 10) and fractionated by SDS–PAGE on 15% gels. The Coomassie blue-stained 17 kDa protein band was excised, in-gel digested with trypsin, and tentatively identified by tandem mass spectrometry as MGST1 along other minor proteins in this band (Figure 2A). On the basis of the primary amino acid sequence and corresponding nucleotide sequence of other species, the complete cDNA of bovine RPE MGST1 was then cloned and sequenced using PCR methods (Figure 2B; deposited in GenBank, accession number AY334548). The bovine MGST1 sequence exhibits 84.5% homology with rat MGST1 and 88.4% homology with human MGST1.

To confirm bovine MGST1 as the immunogen recognized by A1 mAb and not a contaminating protein with similar molecular mass, the recombinant protein was expressed in HEK293 cells and probed by immunoblotting with A1 mAb. The A1 mAb reacted with tetracycline-induced MGST1 in the HEK293 cells (Figure 2C) and with bacterially expressed enzyme (data not shown), verifying the identification of the antigen as MGST1. The mAb against MGST1 did not cross-react with cGST derived from bovine liver (Figure 2C).

Enzyme Activity of MGST1 As Pertaining to Its Possible Physiological Function

MGST1 displays GPx reduction activity against lipid and retinoid peroxidates, a key reaction in the detoxification of the RPE. Both RPE microsomes (Figure 3A) and MGST1 expressed in HEK293 cells (Figure 3B) exhibited GPx activity against 13(*S*)-HpODE, a hydroperoxide derived from linoleic acid. In control experiments, similar activity was observed in the presence of cGST (data not shown). No specific GPx activity was detected in uninduced MGST1-HEK293 cells or in tetracycline-treated HEK293 cells transfected with an empty vector (data not shown). In addition, A1 mAb specifically blocked 53 ± 7% of the GPx activity in the RPE microsomes (Figure 3C). Similarly, the GPx activity of recombinant MGST1 was inhibited by A1 mAb (32 ± 5%). A1 mAb had no significant effect on the GPx activity of the cGSTs mixture (Figure 3C). GPx activity was measured using H_2O_2-treated DHA and RPE microsomes, MGST1, and cGST (Figure 4A), with rates of 2.8 ± 0.5, 3.4± 0.5, and 2.0 ± 0.5 nmol/min, respectively. No GPx activity toward DHA could be detected without H_2O_2 treatment. As predicted, these enzyme preparations were not active against saturated lipid octadecane either treated or untreated with H_2O_2 (Table 1). Because of the structural similarity between retinoids and unsaturated lipids, their importance in RPE physiology, and their susceptibility to oxidative processes (*39*), we also explored the possibility that oxidized retinoids might serve as substrates for GST. Synthetic H_2O_2-treated all-*trans*-retinyl palmitate and all-*trans*-retinol, but not all-*trans*-retinal, were found to undergo GPx reaction rates of 1.1 ± 0.2 and 0.5 ± 0.1 μmol/min, respectively (Figure 4B). In other analyses, cGST, RPE microsomes, and MGST1 displayed 15.4 ± 1.4, 0.06 ± 0.01, and 0.7 ± 0.1 μmol min^{-1} (mg^{-1} of transferase activity), respectively, with CDNB (Table 1). These results suggest that MGST1 is a major enzyme responsible for the detoxification of oxidized products in the RPE. In addition, RPE microsomes were treated with H_2O_2, retinoids were extracted with hexane, and GPx activity was measured. RPE microsomes and recombinant MGST1 displayed initial reaction rates of 3.7 ± 0.5 and 5.0 ± 0.4 nmol/min, respectively (Figure 4B). The GPx reaction rate of cGST was 2.0 ± 0.4 nmol/min, while the control sample lacking GST showed no GPx activity. The main products of the extraction were retinoids such as retinols, retinyl esters, and retinals, although we cannot exclude the possibility that some other hydrophobic compounds were also extracted.

Effect of MGST1 on Cell Viability

MGST1 also appears to increase cell viability when challenged under oxidative stress conditions. At H_2O_2 concentrations between 10 and 40 μM, HEK293 cells expressing MGST1 were more viable than control cells transfected with an empty vector ($P < 0.05$) (Figure 5A). These results were consistent with DNA fragmentation assays (Figure 5B) and with the fact that H_2O_2 induces apoptosis (*40*). Moreover, the cell survival rate of HEK293 cells expressing MGST1 was higher than that of cells transfected with an empty vector challenged with oxidized polyunsaturated fatty acids at concentrations of 60–150 μM (Figure 5C). The levels of lipid peroxides assessed by TBARS showed that MGST1-transfected cells had a significantly reduced amount of lipid peroxides. When 30 μM H_2O_2 was challenged to the cells, MGST1 overexpressing cells produced 0.20 ±0.07 nmol/mg of malondialdehyde (MDA), whereas vector-transfected cells had 0.50 ± 0.09 nmol/mg of MDA (Figure 5D). These results demonstrate that, under the overexpression conditions employed, MGST1 attenuated H_2O_2-induced apoptosis by inhibiting production of lipid peroxides in vitro.

Cell viability was also examined in the presence and absence of H_2O_2 after siRNA inhibition of MGST1 expression. Four targeting siRNA sequences within human MGST1 were selected according to Elbashir et al. (*35–37*) as described in Materials and Methods. Expression was evaluated by immunoblot at different times after siRNA transfection. Transfection of F172 and F264 siRNA inhibited MGST1 expression in ARPE19 cells 24–96 h after treatment as shown by immunoblotting with A1 Ab (Figure 6A), with the largest changes occurring between 48 and 72 h. F172 and F264 siRNA reduced expression of MGST1 by 12% or 26%, respectively, in ARPE19 cells comparable to the control cells transfected with lamin A/C siRNA. In cell viability tests, absorbance of MTT assay indicated 1.8 ± 0.2 or 0.7 ± 0.2 without/with H_2O_2 stimulation in lamin A/C transfected ARPE19 cells, and cytotoxicity effects of H_2O_2 were observed (Figure 6B, left panel). When the viability of MGST1 siRNA-transfected ARPE19 cells was compared with lamin A/C siRNA transfection in the presence of 30 μM H_2O_2, ARPE19 cells transfected with F172 or F264 siRNA showed less viability (51 ± 7%, 60 ± 6%) than cells transfected with F136 or F143 siRNA (93 ± 6%, 94 ± 6%) (Figure 6B, right panel). Transfection of F136 or F143 siRNA did not reduce MGST1 expression and did not affect cell viability (Figure 6A).

The correlation between the expression level of MGST1 and cell viability was also extended to GPx activity. In ARPE19 cells transfected with F172 siRNA, GPx activity toward 13(*S*)-HpODE was reduced by 44 ± 13% relative to GPx activity in ARPE19 cells without siRNA treatment (Figure 6C). These data suggest that MGST1 may also function in vivo in increasing RPE cell viability under conditions of oxidative stress.

Expression of MGST1 as a Function of Age

We investigated whether GPx activity and MGST1 expression levels fluctuated as a function of age. RPE cells were carefully prepared from the eyecups of mice of two different strains at the ages of 6 weeks, 12 months, and 18 months, and MGST1 was probed with A1 mAb. Expression of MGST1 decreased gradually with age in both C57BL/6 and BALB/c mice, with the most dramatic decline occurring in the C57BL/6 mice between 12 months (3–4-fold reduction) and 18 months (trace amounts only) (Figure 7A). No apparent change was observed in expression levels of membrane-associated protein RPE65. Similar results were obtained from two experiments per time point per mouse strain. GPx activity toward 13(*S*)-HpODE was measured using RPE extracts from 6-week-old and 12-month-old C57BL/6 mice (n = 4 eyes per time point), yielding specific GPx reaction rates of 1.2 ± 0.1 and 0.8 ± 0.1 nmol/min, respectively (Figure 7B). Thus, both GPx activity and MGST1 expression levels were found to decease in mouse RPE with age.

DISCUSSION

Role of MGST1 in the RPE

GSTs are considered to be ubiquitous enzymes, representing ~3% of all microsomal proteins, a high level of expression similar to that in the liver (*17*). Not surprisingly, we found MGST1 to be particularly abundant in the RPE and liver and to constitute a major immunogenic antigen in RPE microsomes. Interestingly, MGST1 is not expressed at significant levels in the neural retina. The RPE comprises a single layer of polarized cells that separates the photoreceptors from their principal blood supply in the choroid. Oxygen pressure is higher in choroidal blood than in normal peripheral tissues (~60 vs ~40 mmHg, respectively) and contains 1–30 μM H_2O_2 (*41*, *42*). Moreover, oxygen consumption is higher in the retina than in most other tissues and 4–5 times higher in old retina than in young retina, yet several enzymes providing protection to oxidative stress are more active in the RPE than in the retina (*43*, *44*). The protective mechanisms in the RPE are therefore crucial to healthy retinal physiology. Our cell survival tests in the presence of an oxidative challenge demonstrate that MGST1 increases RPE

cell viability in vitro, suggesting that MGST1 may also provide RPE protection against oxidative stress in vivo.

The abundance of MGST1 in the RPE underscores its potential importance in oxidative processes in these cells. For example, a major role of the RPE is the phagocytosis and degradation of oxidatively spent rod and cone photoreceptor outer segments, which are unusually rich in DHA-containing lipids, polyunsaturated fatty acids, and retinoids. In this study, MGST1 showed GPx activity not only toward lipid peroxides but also against retinoids such as retinyl palmitate treated with H_2O_2. The structural identity of retinoid substrates generated by H_2O_2 treatment was not established by reverse-phase HPLC or GC/MS; however, retinoids are highly labile and readily oxidizable. Other enzymes in the RPE likely supplement the GPx activity of MGST1, including hGST 5.8, which reportedly provides protection against oxidative stress (*45*). MGST1 may also serve important detoxification functions in the retina through GST activity from hydrophobic electrophiles. We speculate that a significant fraction of the ~0.1 mmol thioethers secreted daily by humans (*14*) may come from the RPE, where MGST1 is so highly expressed.

MGST1 Relation with Aging Processes

Reactive oxygen intermediates are continually generated in cells through processes such as the univalent reduction of O_2, metabolism of xenobiotics by monooxygenases, and phagocytosis. The role of these reactive species in initiating lipid peroxidation may be the most damaging to cells because lipid peroxidation can be propagated by autocatalytic reactions. Indeed, lipid peroxidation has been implicated in atherogenesis (*46*), neurodegenerative diseases (*47*), retinopathy (*48*), diabetic complications (*49*), and AMD (*11*, *12*). The protective role of cGST isozymes against lipid peroxidation in ocular tissues is suggested in cataractogenesis and retinal degeneration (*48*, *50*, *51*) but, above all, in the aging process of the retina and in AMD (*48*, *52*). Antioxidant enzymatic systems in the rat and human retina decrease with age (*53*, *54*). Here, we have demonstrated lower expression of MGST1 and less GPx activity in the in vivo RPE of older mice, suggesting that this enzyme could be responsible for age-related changes and lower oxidative resistance with age.

Although the causes of AMD are not well understood at the molecular level, recent studies suggest that oxidative stress is partly responsible (*11*, *12*, *55*). For example, CEP protein adducts uniquely derived from oxidative fragmentation of DHA are elevated in AMD donor tissues such as RPE/Bruch's membrane/choroids and plasma (*12*). Furthermore, antioxidant vitamins and zinc can slow the progression of AMD for select individuals (*56*). We suggest that the GPx activity of MGST1 toward oxidized DHA may be a key antioxidative defense mechanism in the RPE (*54*).

Polymorphisms of MGST1 may influence the susceptibility of the RPE to drugs, oxidative damage, and AMD (*57*). Interestingly, Toba and Aigaki found that the life span of *Drosophila melanogaster* lacking expression of MGST1 was significantly reduced compared with control flies, suggesting that MGST1 is involved in processes that slow aging (*58*). The role of GSTs in human pathologies was also recently strengthened by the finding that the GSTT1 null genotype is associated with an increased risk for acquired aplastic anemia in children (*59*). In summary, we have identified MGST1 as a dominant protein in the RPE, demonstrated antioxidant functions for the enzyme in vitro and in vivo, and shown that expression levels and GPx activity decease with age in mice. We propose that the detoxifying functions of MGST1 may be pivotal in protecting the RPE/retina from oxidative damage and in slowing the progression of diseases such as AMD in the elderly population.

Acknowledgements

We thank Drs. V. Kuksa, F. Haeseleer, A. Alekseev, G. F. Jang, I. Sokal, Y. Imanishi, T. Maeda, A. Moise, and J. Sun as well as K. West for help during the course of this study, and Rebecca Birdsong for help during manuscript preparation.

References

1. Boulton M, Dayhaw-Barker P. The role of the retinal pigment epithelium: topographical variation and ageing changes. Eye 2001;15:384–389. [PubMed: 11450762]
2. Sun H, Nathans J. The challenge of macular degeneration. Sci Am 2001;285:68–75. [PubMed: 11570044]
3. Organisciak DT, Darrow RM, Barsalou L, Kutty RK, Wiggert B. Circadian-dependent retinal light damage in rats. Invest Ophthalmol Visual Sci 2000;41:3694–3701. [PubMed: 11053264]
4. Organisciak DT, Bicknell IR, Darrow RM. The effects of l- and d-ascorbic acid administration on retinal tissue levels and light damage in rats. Curr Eye Res 1992;11:231–241. [PubMed: 1587146]
5. Organisciak DT, Jiang YL, Wang HM, Bicknell I. The protective effect of ascorbic acid in retinal light damage of rats exposed to intermittent light. Invest Ophthalmol Visual Sci 1990;31:1195–1202. [PubMed: 2365553]
6. Sun H, Nathans J. ABCR, the ATP-binding cassette transporter responsible for Stargardt macular dystrophy, is an efficient target of all-trans-retinal-mediated photooxidative damage in vitro. Implications for retinal disease. J Biol Chem 2001;276:11766–11774. [PubMed: 11278627]
7. McBee JK, Van Hooser JP, Jang GF, Palczewski K. Isomerization of 11-cis-retinoids to all-trans-retinoids in vitro and in vivo. J Biol Chem 2001;276:48483–48493. [PubMed: 11604395]
8. Noell WK, Albrecht R. Irreversible effects on visible light on the retina: role of vitamin A. Science 1971;172:76–79. [PubMed: 5546288]
9. Saari JC, Nawrot M, Kennedy BN, Garwin GG, Hurley JB, Huang J, Possin DE, Crabb JW. Visual cycle impairment in cellular retinaldehyde binding protein (CRALBP) knockout mice results in delayed dark adaptation. Neuron 2001;29:739–748. [PubMed: 11301032]
10. Sieving PA, Chaudhry P, Kondo M, Provenzano M, Wu D, Carlson TJ, Bush RA, Thompson DA. Inhibition of the visual cycle in vivo by 13-cis retinoic acid protects from light damage and provides a mechanism for night blindness in isotretinoin therapy. Proc Natl Acad Sci USA 2001;98:1835–1840. [PubMed: 11172037]
11. Gu X, Meer SG, Miyagi M, Rayborn ME, Hollyfield JG, Crabb JW, Salomon RG. Carboxyethylpyrrole protein adducts and autoantibodies, biomarkers for age-related macular degeneration. J Biol Chem 2003;278:42027–42035. [PubMed: 12923198]
12. Crabb JW, Miyagi M, Gu X, Shadrach K, West KA, Sakaguchi H, Kamei M, Hasan A, Yan L, Rayborn ME, Salomon RG, Hollyfield JG. Drusen proteome analysis: an approach to the etiology of age-related macular degeneration. Proc Natl Acad Sci USA 2002;99:14682–14687. [PubMed: 12391305]
13. Mukherjee PK, Marcheselli VL, Serhan CN, Bazan NG. Neuroprotectin D1: a docosahexaenoic acid-derived docosatriene protects human retinal pigment epithelial cells from oxidative stress. Proc Natl Acad Sci USA 2004;101:8491–8496. [PubMed: 15152078]
14. Rinaldi R, Eliasson E, Swedmark S, Morgenstern R. Reactive intermediates and the dynamics of glutathione transferases. Drug Metab Dispos 2002;30:1053–1058. [PubMed: 12228179]
15. Vuilleumier S, Pagni M. The elusive roles of bacterial glutathione S-transferases: new lessons from genomes. Appl Microbiol Biotechnol 2002;58:138–146. [PubMed: 11876405]
16. Mannervik B, Awasthi YC, Board PG, Hayes JD, Di Ilio C, Ketterer B, Listowsky I, Morgenstern R, Muramatsu M, Pearson WR, et al. Nomenclature for human glutathione transferases. Biochem J 1992;282:305–306. [PubMed: 1540145]
17. Andersson C, Mosialou E, Weinander R, Morgenstern R. Enzymology of microsomal glutathione S-transferase. Adv Pharmacol 1994;27:19–35. [PubMed: 8068553]
18. Pickett CB, Lu AY. Glutathione S-transferases: gene structure, regulation, and biological function. Annu Rev Biochem 1989;58:743–764. [PubMed: 2673020]

19. Jakobsson PJ, Morgenstern R, Mancini J, Ford-Hutchinson A, Persson B. Membrane-associated proteins in eicosanoid and glutathione metabolism (MAPEG). A widespread protein superfamily. Am J Respir Crit Care Med 2000;161:S20–S24. [PubMed: 10673221]
20. Townsend DM, Tew KD. The role of glutathione-S-transferase in anti-cancer drug resistance. Oncogene 2003;22:7369–7375. [PubMed: 14576844]
21. Jakobsson PJ, Morgenstern R, Mancini J, Ford-Hutchinson A, Persson B. Common structural features of MAPEG—a widespread superfamily of membrane associated proteins with highly divergent functions in eicosanoid and glutathione metabolism. Protein Sci 1999;8:689–692. [PubMed: 10091672]
22. Kelner MJ, Bagnell RD, Montoya MA, Estes LA, Forsberg L, Morgenstern R. Structural organization of the microsomal glutathione S-transferase gene (MGST1) on chromosome 12p13.1–13.2. Identification of the correct promoter region and demonstration of transcriptional regulation in response to oxidative stress. J Biol Chem 2000;275:13000–13006. [PubMed: 10777602]
23. Holm PJ, Morgenstern R, Hebert H. The 3-D structure of microsomal glutathione transferase 1 at 6 Å resolution as determined by electron crystallography of p22(1)2(1) crystals. Biochim Biophys Acta 2002;1594:276–285. [PubMed: 11904223]
24. Schmidt-Krey I, Mitsuoka K, Hirai T, Murata K, Cheng Y, Fujiyoshi Y, Morgenstern R, Hebert H. The three-dimensional map of microsomal glutathione transferase 1 at 6 Å resolution. EMBO J 2000;19:6311–6316. [PubMed: 11101503]
25. Palczewski K, Buczylko J, Lebioda L, Crabb JW, Polans AS. Identification of the N-terminal region in rhodopsin kinase involved in its interaction with rhodopsin. J Biol Chem 1993;268:6004–6013. [PubMed: 8383684]
26. Saari JC, Bredberg DL. Acyl-CoA:retinol acyltransferase and lecithin:retinol acyltransferase activities of bovine retinal pigment epithelial microsomes. Methods Enzymol 1990;190:156–163. [PubMed: 2087167]
27. Papermaster DS. Preparation of antibodies to rhodopsin and the large protein of rod outer segments. Methods Enzymol 1982;81:240–246. [PubMed: 6212740]
28. Bradford MM. A rapid and sensitive method for the quantitation of microgram quantities of protein utilizing the principle of protein-dye binding. Anal Biochem 1976;72:248–254. [PubMed: 942051]
29. Adamus G, Zam ZS, Arendt A, Palczewski K, McDowell JH, Hargrave PA. Anti-rhodopsin monoclonal antibodies of defined specificity: characterization and application. Vision Res 1991;31:17–31. [PubMed: 2006550]
30. Laemmli UK. Cleavage of structural proteins during the assembly of the head of bacteriophage T4. Nature 1970;227:680–685. [PubMed: 5432063]
31. Ohguro H, Chiba S, Igarashi Y, Matsumoto H, Akino T, Palczewski K. Beta-arrestin and arrestin are recognized by autoantibodies in sera from multiple sclerosis patients. Proc Natl Acad Sci USA 1993;90:3241–3245. [PubMed: 8475065]
32. Habig WH, Pabst MJ, Jakoby WB. Glutathione S-transferases. The first enzymatic step in mercapturic acid formation. J Biol Chem 1974;249:7130–7139. [PubMed: 4436300]
33. Yang Y, Cheng JZ, Singhal SS, Saini M, Pandya U, Awasthi S, Awasthi YC. Role of glutathione S-transferases in protection against lipid peroxidation. Overexpression of hGSTA2–2 in K562 cells protects against hydrogen peroxide-induced apoptosis and inhibits JNK and caspase 3 activation. J Biol Chem 2001;276:19220–19230. [PubMed: 11279091]
34. West KA, Yan L, Shadrach K, Sun J, Hasan A, Miyagi M, Crabb JS, Hollyfield JG, Marmorstein AD, Crabb JW. Protein database, human retinal pigment epithelium. Mol Cell Proteomics 2003;2:37–49. [PubMed: 12601081]
35. Elbashir SM, Harborth J, Lendeckel W, Yalcin A, Weber K, Tuschl T. Duplexes of 21-nucleotide RNAs mediate RNA interference in cultured mammalian cells. Nature 2001;411:494–498. [PubMed: 11373684]
36. Elbashir SM, Lendeckel W, Tuschl T. RNA interference is mediated by 21- and 22-nucleotide RNAs. Genes Dev 2001;15:188–200. [PubMed: 11157775]
37. Elbashir SM, Martinez J, Patkaniowska A, Lendeckel W, Tuschl T. Functional anatomy of siRNAs for mediating efficient RNAi in *Drosophila melanogaster* embryo lysate. EMBO J 2001;20:6877–6888. [PubMed: 11726523]

38. Wagner BA, Buettner GR, Oberley LW, Darby CJ, Burns CP. Myeloperoxidase is involved in H2O2-induced apoptosis of HL-60 human leukemia cells. J Biol Chem 2000;275:22461–22469. [PubMed: 10801811]
39. Nagao A. Oxidative conversion of carotenoids to retinoids and other products. J Nutr 2004;134:237S–240S. [PubMed: 14704326]
40. Hockenbery DM, Oltvai ZN, Yin XM, Milliman CL, Korsmeyer SJ. Bcl-2 functions in an antioxidant pathway to prevent apoptosis. Cell 1993;75:241–251. [PubMed: 7503812]
41. Garcia-Castineiras S, Velazquez S, Martinez P, Torres N. Aqueous humor hydrogen peroxide analysis with dichlorophenol-indophenol. Exp Eye Res 1992;55:9–19. [PubMed: 1397135]
42. Spector A, Ma W, Wang RR. The aqueous humor is capable of generating and degrading H_2O_2. Invest Ophthalmol Visual Sci 1998;39:1188–1197. [PubMed: 9620079]
43. Cohen LH, Noell WK. Glucose catabolism of rabbit retina before and after development of visual function. J Neurochem 1960;5:253–276. [PubMed: 13810977]
44. Hess R, Pearse AG. Histochemical demonstration of uridine diphosphate glucose dehydrogenase. Experientia 1961;17:317–318. [PubMed: 13713927]
45. Singhal SS, Godley BF, Chandra A, Pandya U, Jin GF, Saini MK, Awasthi S, Awasthi YC. Induction of glutathione S-transferase hGST 5.8 is an early response to oxidative stress in RPE cells. Invest Ophthalmol Visual Sci 1999;40:2652–2659. [PubMed: 10509662]
46. Witztum JL. The oxidation hypothesis of atherosclerosis. Lancet 1994;344:793–795. [PubMed: 7916078]
47. Kruman I, Bruce-Keller AJ, Bredesen D, Waeg G, Mattson MP. Evidence that 4-hydroxynonenal mediates oxidative stress-induced neuronal apoptosis. J Neurosci 1997;17:5089–5100. [PubMed: 9185546]
48. Armstrong D, Hiramitsu T. Studies of experimentally induced retinal degeneration: 2. Early morphological changes produced by lipid peroxides in the albino rabbit. Jpn J Ophthalmol 1990;34:158–173. [PubMed: 2214359]
49. Ansari NH, Zhang W, Fulep E, Mansour A. Prevention of pericyte loss by trolox in diabetic rat retina. J Toxicol Environ Health A 1998;54:467–475. [PubMed: 9661912]
50. Srivastava SK, Singhal SS, Awasthi S, Pikula S, Ansari NH, Awasthi YC. A glutathione S-transferases isozyme (bGST 5.8) involved in the metabolism of 4-hydroxy-2-trans-nonenal is localized in bovine lens epithelium. Exp Eye Res 1996;63:329–337. [PubMed: 8943706]
51. Babizhayev MA. Failure to withstand oxidative stress induced by phospholipid hydroperoxides as a possible cause of the lens opacities in systemic diseases and ageing. Biochim Biophys Acta 1996;1315:87–99. [PubMed: 8608175]
52. Cohen SM, Olin KL, Feuer WJ, Hjelmeland L, Keen CL, Morse LS. Low glutathione reductase and peroxidase activity in age-related macular degeneration. Br J Ophthalmol 1994;78:791–794. [PubMed: 7803358]
53. Castorina C, Campisi A, Di Giacomo C, Sorrenti V, Russo A, Vanella A. Lipid peroxidation and antioxidant enzymatic systems in rat retina as a function of age. Neurochem Res 1992;17:599–604. [PubMed: 1603266]
54. Naash MI, Nielsen JC, Anderson RE. Regional distribution of glutathione peroxidase and glutathione-S-transferase in adult and premature human retinas. Invest Ophthalmol Visual Sci 1988;29:149–152. [PubMed: 3335428]
55. Evans JR. Risk factors for age-related macular degeneration. Prog Retinal Eye Res 2001;20:227–253.
56. Snodderly DM. Evidence for protection against age-related macular degeneration by carotenoids and antioxidant vitamins. Am J Clin Nutr 1995;62:1448S–1461S. [PubMed: 7495246]
57. Hayes JD, Strange RC. Glutathione S-transferase polymorphisms and their biological consequences. Pharmacology 2000;61:154–166. [PubMed: 10971201]
58. Toba G, Aigaki T. Disruption of the microsomal glutathione S-transferase-like gene reduces life span of *Drosophila melanogaster*. Gene 2000;253:179–187. [PubMed: 10940555]
59. Dirksen U, Moghadam KA, Mambetova C, Esser C, Fuhrer M, Burdach S. Glutathione S transferase theta 1 gene (GSTT1) null genotype is associated with an increased risk for acquired aplastic anemia in children. Pediatr Res 2004;55:466–471. [PubMed: 14681495]

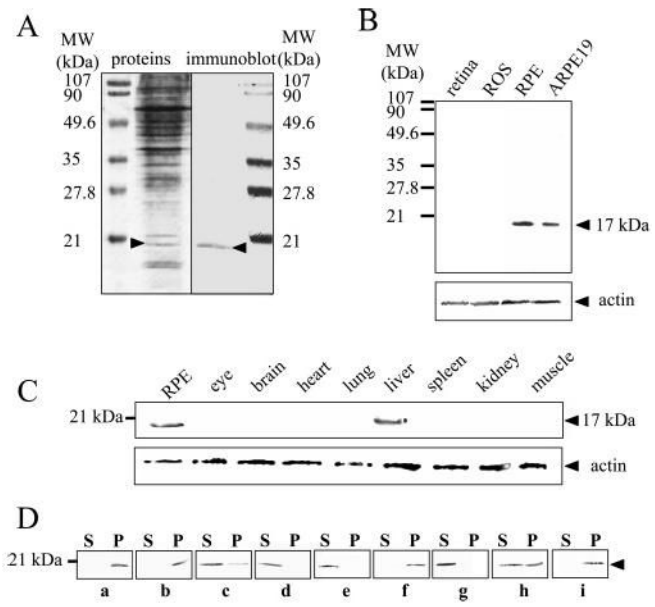

Figure 1.

Microsomal antigen recognized by A1 mAb in the RPE and other tissues. (A) Microsomal proteins (5 μg) from bovine RPE were separated by 15% SDS–PAGE, and the gel was stained with Coomassie blue (left panel). A 17 kDa band was visualized by immunoblotting (right panel) using A1 mAb. SDS–PAGE, immunoblotting procedures, and preparation of RPE microsomes and A1 mAb are described in Materials and Methods. A longer exposure of the immunoblot did not reveal any band other than the 17 kDa antigen. (B) Expression of the 17 kDa antigen in the eye and in ARPE19 cells. Proteins from bovine retina, bovine rod outer segment (ROS), bovine RPE microsomes, and human RPE cultured cells (ARPE19) were extracted using SDS sample buffer (50 μg each) and probed by immunoblotting with A1 mAb. The 17 kDa antigen was found in the RPE microsomes and ARPE19 cells but not in the retina and ROS. The equal loading of the sample was verified by immunoblotting with anti-actin pAb. Three independent experiments yielded similar results. (C) Expression of the 17 kDa antigen in the RPE and in other organs. Indicated organs from a BALB/c mouse were homogenized and washed three times with 100 mM Na_2CO_3 (pH 10), and pellets were collected by centrifugation at 275000*g*. The expression of the 17 kDa protein was probed with A1 mAb. The equal loading of the sample was verified by immunoblotting with anti-actin pAb. Three independent experiments yielded similar results. (D) Solubility of the 17 kDa antigen protein. Bovine RPE microsomes (50 μg) were suspended in the different extraction solutions (below); soluble and insoluble proteins were separated by centrifugation. The solubility of the 17 kDa antigen was examined by immunoblotting with A1 mAb. S is the soluble fraction, and P is the pellet fraction. The following solutions were used: (a) 100 mM K_2CO_3 (pH 10); (b) 50 mM K_2CO_3 and 5 mM DM (pH 10); (c) 10 mM DM; (d) 4 M urea and 5 mM DM; (e) 8 M urea; (f) 2 M NH_4Cl; (g) 1% SDS; (h) 25 mM CHAPS; and (i) H_2O. The 17 kDa antigen was solubilized only in the presence of detergent, suggesting it is a microsomal protein. Three independent experiments yielded similar results.

A

Query	m/z	charge	MW	Delta	start	end	sequence
13	513.91	3	1538.7	-0.024	42	55	KVFANPEDCAGFGK
59	706.31	2	1410.6	-0.016	43	55	VFANPEDCAGFGK
56	637.62	3	1909.9	-0.029	43	60	VFANPEDCAGFGKGENAK
29	949.1	2	1896	-0.014	115	130	IYHTIAYLTPLPQPNR

B

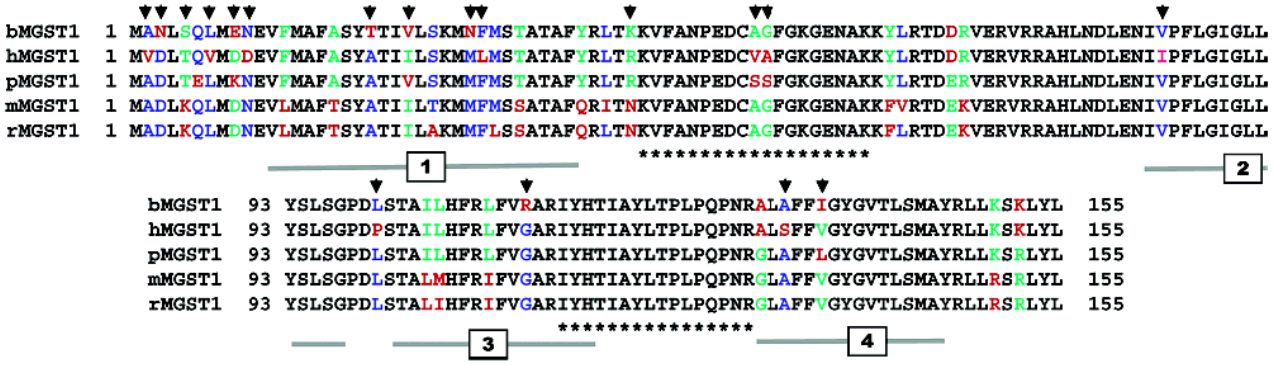

C

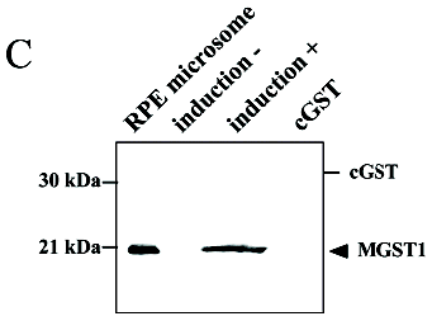

Figure 2.

Identification of the 17 kDa antigen from RPE microsomes by liquid chromatography/mass spectrometry (LC MS/MS) and immunoreactivity with recombinant MGST1. (A) LC MS/MS analysis of identified peptides from the 17 kDa antigen. (B) Cloning of bovine MGST1 and amino acid sequence alignment with MGST1 from several species (b, bovine; h, human; p, pig; m, mouse; r, rat). The identical residues are in black letters; residues that are preset in three or four species are shown in green and blue, respectively; in red are residues that occur only once or twice among analyzed species. Asterisks indicate the sequence obtained by the in-gel cleavage and LC MS/MS analysis. Transmembrane segments (*23*) are numbered and indicated by the gray bars. (C) Immunoreactivity of A1 mAb with recombinant MSGT1 and GSTs from bovine liver. Bovine MGST1 was stably expressed in the HEK293 cells, using the tetracycline-inducible Invitrogen T-Rex system as described in Materials and Methods. Expression of MGST1 (10 μg of total proteins) was probed by immunoblotting with A1 mAb. The expected molecular mass of bovine cGST and MGST1 is indicated on the right. A1 mAb did not cross-react with cGST. Three independent experiments yielded similar results.

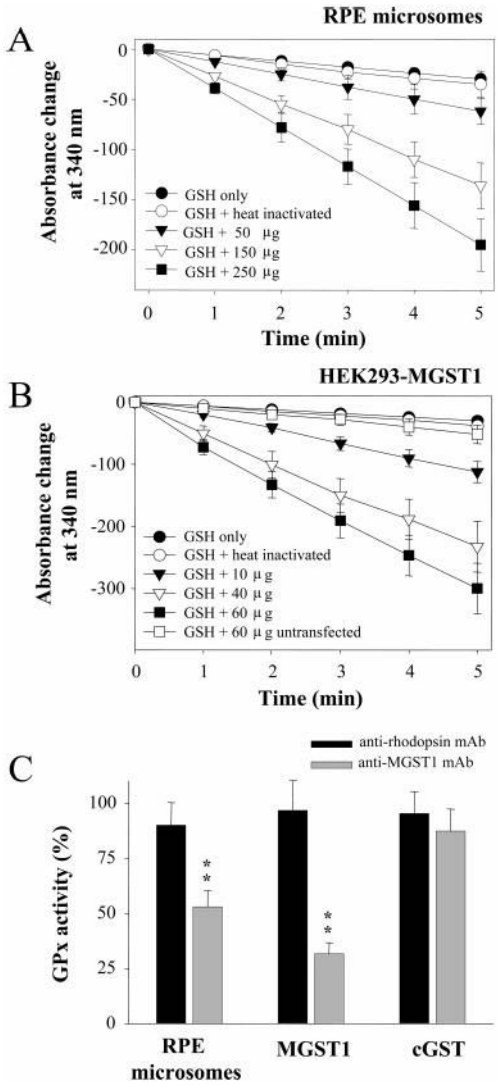

Figure 3.

GPx assay and inhibition of GPx activity in the RPE microsomes by A1 (anti-MGST1) mAb. (A) Time course of GPx activity using different amounts of bovine RPE microsomes (0–250 μg) activated by 0.1% Triton X-100 as a source of GST. The reaction mixture containing 3.2 mM GSH, 0.32 mM NADPH, 1 unit of GR, and 0.82 mM EDTA in 0.16 M Tris (pH 7.0) was preincubated with activated RPE, and the reaction was initiated by addition of 100 μM 13(*S*)-HpODE (final concentration) and monitored as a change of absorption at 340 nm. The assay conditions are described in Materials and Methods. The mean ± SEM of five determinations is shown. (B) Time course of GPx activity using different amounts of recombinant MGST1 expressed in HEK293 membranes (0–60 μg) activated by 0.1% Triton X-100 as a source of GST. The reaction mixture containing 3.2 mM GSH, 0.32 mM NADPH, 1 unit of GR, and 0.82 mM EDTA in 0.16 M Tris (pH 7.0) was preincubated with activated membrane, and the reaction was initiated by addition of 100 μM 13(*S*)-HpODE (final concentration) and monitored as a change of absorption at 340 nm. The mean ± SEM of five determinations is shown. (C) Inhibition of GPx activity by A1 (anti-MGST1) mAb. Fifty micrograms of A1 mAb or unrelated mouse anti-rhodopsin was preincubated for 30 min on ice with 1 μg of cGST, 100 μg of Triton X-100-activated RPE microsomes, and 10 μg of Triton X-100-activated MGST1

expressed in HEK293 cells. GPx activity was examined, and activities were normalized to the controls. Results are the means ± SEM of five determinations. Key: $^{**}P < 0.01$.

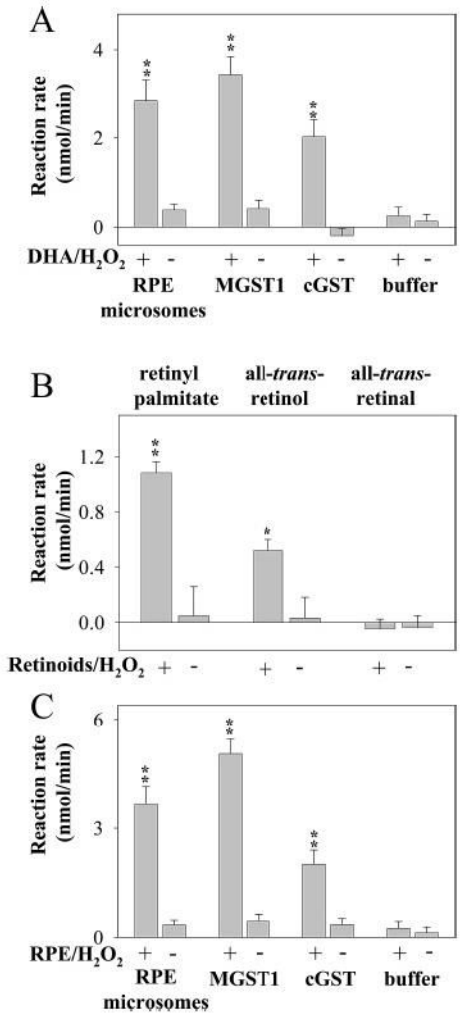

Figure 4.

GPx activity toward H_2O_2-treated DHA, native RPE, and synthetic retinoids. (A) GPx activity using H_2O_2-treated (+) DHA (150 μM) as hydroperoxide substrates (see Materials and Methods). Triton X-100-activated RPE microsomes (100 μg/mL), Triton X-100-activated MGST1 from HEK293 cell membranes (10 μg/mL), and cGST (1 μg/mL) in the presence (+) or absence (−) of H_2O_2-treated DHA (150 μM) were used. The mean ± SEM of five determinations is shown. In control experiments, (1) the reaction mixture minus membranes and (2) H_2O_2-untreated (−) DHA (150 μM) were employed. Key: $^{**}P < 0.01$. (B) GPx activity using H_2O_2-treated (+) retinoids (150 μM) as hydroperoxide substrates. Purified retinyl palmitate, all-*trans*-retinol, and all-*trans*-retinal were exposed to H_2O_2, and GPx activities of Triton X-100-activated MGST1 from HEK293 cell membranes (10 μg/mL) were examined. The mean ± SEM of five determinations is shown. Key: $^{**}P < 0.01$; $^{*}P < 0.05$. All-*trans*-retinyl esters and all-*trans*-retinol, but not all-*trans*-retinal, generated GPx substrate(s) after H_2O_2 treatment. In control experiments H_2O_2-untreated retinoids were employed. (C) GPx activity using retinoids extracted from H_2O_2-treated (+) RPE microsomes (500 μg) as hydroperoxide substrates (see Materials and Methods). Retinoids were extracted from the RPE microsomes with 500 μL of hexane and dried with argon. Triton X-100-activated RPE microsomes (100 μg/mL), Triton X-100-activated MGST1 from HEK293 cell membranes (10 μg/ mL), and cGST (1 μg/mL) were used. The mean ± SEM of five determinations is shown.

In control experiments, (1) the reaction mixture minus membranes and (2) retinoids from H_2O_2-untreated (−) RPE (500 μg) were employed. Key: $^{**}P < 0.01$.

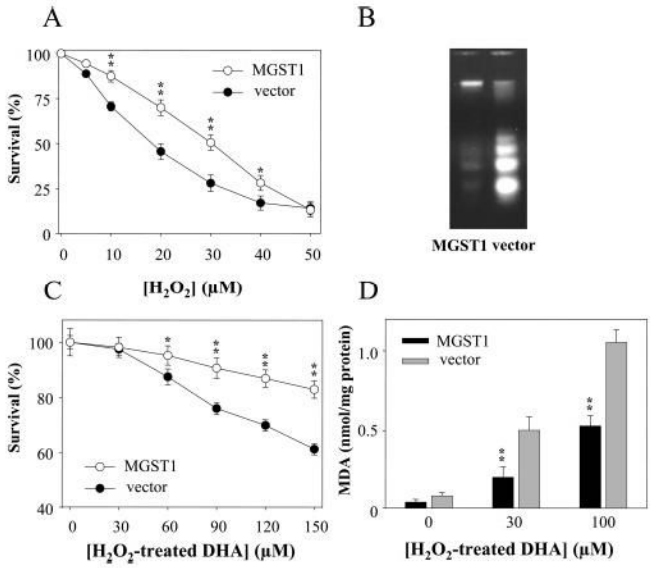

Figure 5.

Cytotoxic effect of H_2O_2 and H_2O_2-treated DHA on HEK293 cells transfected with MGST1. (A) Cytotoxic effect of H_2O_2 on HEK293 cells transfected with MGST1. After 48 h induction by 1 μg/mL tetracycline, MGST1- or control vector-transfected HEK293 cells were seeded into five replicate wells at a concentration of 3 × 104 with various H_2O_2 concentrations (0–50 μM) in a 96-well plate and incubated for 48 h. The cytotoxic effect of H_2O_2 was examined by MTT assay as described in Materials and Methods. The control reference cells (100% survival) were untreated with H_2O_2. Representative results from one of the four independent experiments on H_2O_2 cytotoxicity are presented. Key: error bars, SEM; $^{**}P < 0.01$; $^{*}P < 0.05$. (B) DNA fragmentation. This figure shows DNA fragmentation after H_2O_2 treatment of HEK293 cells either expressing MGST1 or containing empty vector. HEK293 cells were treated with 30 μM H_2O_2 for 48 h. After the incubations, genomic DNA was extracted and run on a 2% agarose gel. Apoptosis was examined by the appearance of characteristic DNA laddering. (C) Cytotoxic effect of H_2O_2-treated DHA on HEK293 cells transfected with MGST1. After 48 h induction by 1 μg/mL tetracycline, MGST1 or vector-transfected HEK293 cells were seeded into five replicate wells at a concentration of 3 × 104 with various H_2O_2-treated DHA concentrations (0–150 μM) in a 96-well plate and incubated for 24 h. DHA was treated with 395 mM H_2O_2 as described in Materials and Methods. The cytotoxic effect of H_2O_2 was examined by MTT assay as described in Materials and Methods. The control reference cells (100% survival) were untreated with H_2O_2. Representative results from one of the four independent experiments on H_2O_2 cytotoxicity are presented. Key: error bars, SEM; $^{**}P < 0.01$; $^{*}P < 0.05$. (D) Effect on lipid peroxide. After 48 h induction by 1 μg/mL tetracycline, MGST1- or control vector-transfected HEK293 cells were seeded into three replicate plates at a concentration of 3 × 10^7 with various H_2O_2 concentrations (0–60 μM) and incubated for 48 h. Lipid peroxide levels were determined by thiobarbituric acid-reactive substances (TABRS) as described in Materials and Methods. Key: error bars, SEM; $^{**}P < 0.01$.

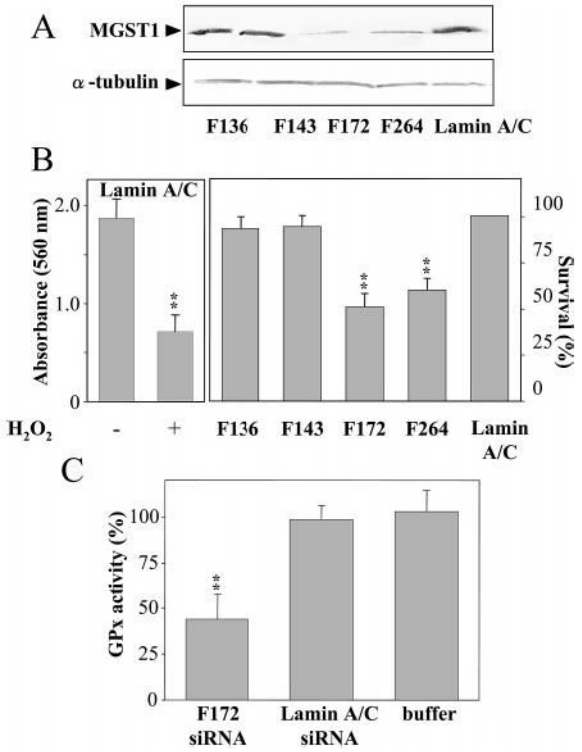

Figure 6.

Effects of RNA interference on cell survival and MGST1 activity. (A) Immunoblotting analysis of MGST1 expression by A1 mAb. ARPE19 cells were transfected with different siRNAs from the MGST1 sequence as described in Materials and Methods. The expression levels of MGST1 after 48 h posttransfection were detected by immunoblotting with A1 MGST1 mAb. The equal loading of the sample was verified by immunoblotting with anti-α-tubulin pAb. (B) Survival assay of ARPE19 cells transfected with different siRNAs. The level of cell survival under 30 μM H_2O_2 stress for 48 h was examined by MTT assay as described in Materials and Methods. Left panel: Absorbance from MTT assay of lamin A/C siRNA-transfected ARPE19 cells with/without H_2O_2 is presented. Right panel: Survival rate of MGST1-derived siRNA-transfected ARPE19 cells under 30 μM H_2O_2 stress is shown. A_{560} values were normalized to cells without H_2O_2 treatment and then compared with lamin A/C siRNA-transfected cells that showed silencing expression of the protein (*35–37*). Representative results from one of the four independent experiments on H_2O_2 cytotoxicity are presented. Key: error bars, SEM; $^{**}P < 0.01$. (C) GPx activity of siRNA transfected ARPE19 cells was examined 48 h after transfection. Microsomes were prepared as described in Materials and Methods, and GPx activity toward 100 μM 13(S)-HpODE was analyzed. Triton X-activated microsomes (100 μg) were used for the assay. GPx activities were normalized to control ARPE19 microsomes without siRNA transfection. Representative results from one of the four independent experiments on H_2O_2 cytotoxicity are presented. Key: error bars, SEM; $^{**}P < 0.01$.

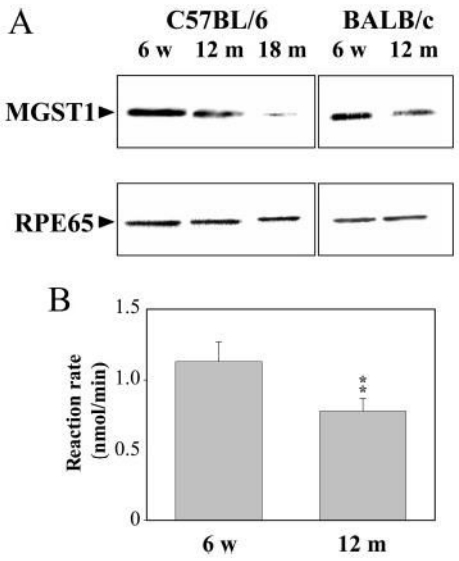

Figure 7.

MGST1 expression in young and old mice. (A) Mouse RPE extract was prepared as described in Materials and Methods. The extract equivalent of one eye was analyzed by immunoblotting with A1 mAb and anti-RPE65 pAb. Antibody binding was detected with the ECL system (Pharmacia) as described in Materials and Methods. The expression of MGST1 was probed with A1 mAb. Similar results were obtained in two independent experiments. (B) GPx activity of mouse RPE. C57BL/6 mouse RPE was prepared as described in Materials and Methods. GPx activity of Triton X-activated RPE toward 100 μM 13(*S*)-HpODE was analyzed (see Materials and Methods). The equivalent of four eyes was used in these experiments. The mean ± SEM of three determinations is shown. Key: $^{**}P < 0.01$.

Table 1

GPx and GST Activities of RPE Microsomes and Recombinant MGST1[a]

activity	substrate	specific activity (μmol min^{-1} mg^{-1})			
		cGST	RPE microsomes	MGST1[c]	vector alone[c]
GPx	13(*S*)-HpODE	8.1 ± 0.6	0.03 ± 0.005	0.35 ± 0.06	ND[b]
	DHA[c]	2.8 ± 0.5	0.03 ± 0.005	0.34 ± 0.05	ND[b]
	DHA	ND[b]	ND[b]	ND[b]	ND[b]
	retinoids[d]	2.0 ± 0.4	0.04 ± 0.005	0.50 ± 0.04	ND[b]
	retinoids	ND[b]	ND[b]	ND[b]	ND[b]
	octadecane[d]	ND[b]	ND[b]	ND[b]	ND[b]
	octadecane	ND[b]	ND[b]	ND[b]	ND[b]
GST	CDNB	15.4 ± 1.4	0.06 ± 0.01	0.7 ± 0.1	ND

[a] The reactions were carried out as described in Materials and Methods.

[b] ND, not detected.

[c] Cell membranes of transfected HEK293 cells.

[d] H_2O_2 treated.